J|A|C|S COMMUNICATIONS

Published on Web 01/14/2009

Polyhedral Au Nanocrystals Exclusively Bound by {110} Facets: The Rhombic Dodecahedron

Gyoung Hwa Jeong,[†] Minjung Kim,[†] Young Wook Lee,[†] Wonjun Choi,[‡] Won Taek Oh,[‡] Q-Han Park,[‡] and Sang Woo Han*,[†]

Department of Chemistry, Research Institute of Natural Science, Environmental Biotechnology National Core Research Center, Gyeongsang National University, Jinju 660-701, Korea, and Department of Physics, Korea University, Seoul 136-701, Korea

Received November 21, 2008; E-mail: swhan@gnu.ac.kr

The synthesis of metal nanocrystals with various geometries has been a very important issue because their optical, electronic, and magnetic properties can be tuned by controlling their size and shape.[1] In particular, the activity of metal nanocrystals in chemical reaction highly depends on their surface properties which are influenced by the shape of synthesized nanocrystals.[2] Accordingly, a number of face-centered cubic (fcc) structured noble metal nanocrystals have been synthesized. Although there are few reports on the preparation of nanocrystals with exposed high-index facets,[3] most of the synthesized nanocrystals are enclosed by low-index {111} and {100} surfaces. For instance, tetrahedral,[4] octahedral,[5] decahedral,[6] and icosahedral[7] nanocrystals are bound by {111} surfaces, and nanocubes[8] are enclosed by {100} surfaces. In addition, cuboctahedral nanocrystals and nanoplates are bound by both {111} and {100} surfaces.[9] On the basis of the fact that surface energies of different crystallographic planes are in the order $\gamma_{\{111\}} < \gamma_{\{100\}} < \gamma_{\{110\}}$,[10] the formation of these structures can be ascribed to a result of the minimization of surface energy.

Up to now, metal nanocrystals exclusively enclosed by {110} surfaces, like rhombic dodecahedron or regular dodecahedron, have been rarely exploited[11] because the {110} facet has the highest surface energy among the low-index facets, thus exhibiting faster growth kinetics over the other facets, resulting in their disappearance during the crystal growth.[12] It is widely accepted that the synthesis of metal nanocrystals with exposed high-energy facets is an important and challenging task because these facets can endow nanocrystals with a high activity, thus facilitating their potential applications such as highly efficient catalysts.[3] Herein, we report on the synthesis of rhombic dodecahedral Au nanocrystals in high yield by a simple wet chemical method. The Au nanocrystals enclosed by 12 {110} facets could be readily prepared without the use of any seeds, surfactants, or foreign metal ions but only with *N*,*N*-dimethylformamide (DMF) as both reductant and solvent.

In a typical synthesis of rhombic dodecahedral Au nanocrystals, an aqueous solution of $HAuCl_4$ (10 mM, 2.0 mL) was added to 23.0 mL of DMF. This solution was then heated at 90−95 °C for ∼15 h in an oven. The resultant sample was purified by centrifugation and washing with ethanol to remove excess reagents. Figure 1a shows a representative SEM image of the as-prepared product. A high-magnification SEM image is also shown in Figure 1b. The images show that the majority (>85%) of the sample was rhombic dodecahedral nanocrystals with an average edge length of 138 ± 21 nm. Some irregularly shaped particles are also observed, which are byproducts of the reaction. The prepared Au nanocrystals were stable up to 2 months under ambient condition. An ideal rhombic dodecahedral structure bound by 12 {110} surfaces presented in Figure 1c correlates well with the synthesized nanocrystals. It is noticeable that the X-ray diffraction (XRD) pattern of the product shows an overwhelmingly intense peak from the (220) diffraction plane with a weak peak from the (111) plane of fcc Au (JCPDS No. 4−0784). The intensity ratio between the (220) and the (111) diffractions ($I_{(220)}/I_{(111)}$) of 12.1 for the prepared sample is remarkably higher than the conventional bulk intensity ratio (0.32), indicating that the faces of these nanocrystals are primarily composed of {110} planes.

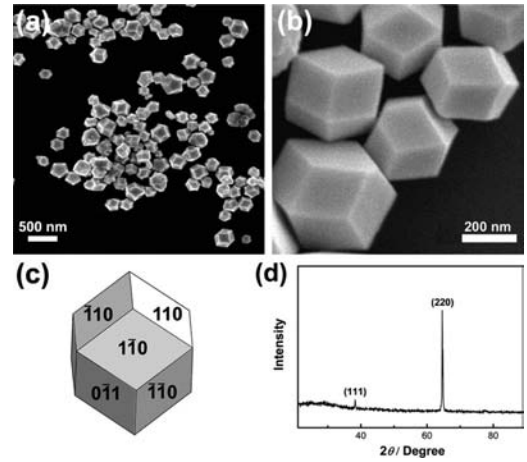

Figure 1. (a) Low- and (b) high-magnification SEM images of the rhombic dodecahedral Au nanocrystals. (c) An ideal rhombic dodecahedron enclosed by 12 {110} facets. (d) XRD pattern of the rhombic dodecahedral Au nanocrystals.

The crystal structure of the prepared nanocrystals was further confirmed by high-resolution transmission electron microscopy (HRTEM) measurements. Figure 2a shows an HRTEM image of the nanocrystals, and the top-right inset shows the selected area electron diffraction (SAED) pattern obtained from a single rhombic dodecahedron with the electron beam perpendicular to one of the rhombic facets. The SAED pattern can be indexed to the [011] zone axis of a single crystal of fcc Au,[13] indicating that the synthesized nanocrystals are single-crystalline and bound by {110} basal planes. The high-magnification HRTEM image also demonstrates the exposed surface of the {110} face (Figure 2b); a *d*-spacing of 0.144 nm for adjacent lattice planes corresponds to the {110} planes of fcc Au.

The electrochemical behavior of the prepared nanocrystals has also been characterized to examine their surface properties. The cyclic voltammetry (CV) trace of rhombic dodecahedral Au nanocrystals immobilized on an indium−tin oxide electrode cor-

[†] Gyeongsang National University.
[‡] Korea University.

10.1021/ja809112n CCC: $40.75

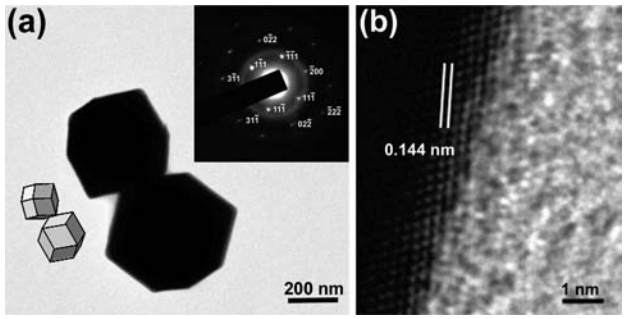

Figure 2. (a) TEM image of the rhombic dodecahedral Au nanocrystals. Top-right inset shows corresponding SAED pattern. Models of ideal rhombic dodecahedra are shown in bottom-left inset. (b) High-magnification HRTEM image of a nanocrystal.

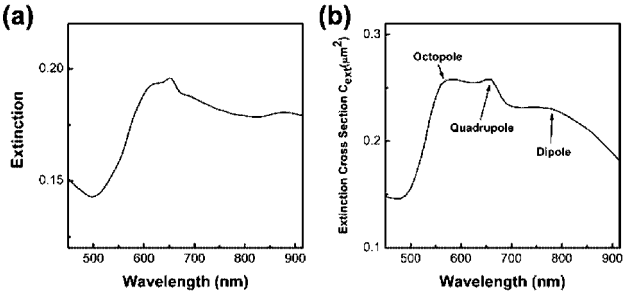

Figure 3. Experimentally measured (a) and calculated (b) extinction spectra of the rhombic dodecahedral Au nanocrystals.

related well with the results obtained from the bulk Au(110) single-crystal electrode and was different from that of the Au nanocrystals bounded by other low-index facets (Figure S1). This result indicates that the synthesized nanocrystals are enclosed by single-crystalline {110} surfaces as revealed by XRD and HRTEM measurements.

The metal nanocrystals with well-defined morphologies exhibit distinct optical properties associated with the surface plasmons.[1] Figure 3a shows the extinction spectrum of the as-prepared Au nanocrystals in DMF. To verify the experimentally observed result, the extinction properties of a nanocrystal (140 nm in edge length) have been computed using the discrete dipole approximation (DDA)[14] and analyzed by comparing the calculated extinction spectrum with the analytic solution of Mie scattering for a similar spherical structure. The calculated extinction spectrum is given in Figure 3b which shows peaks corresponding to dipole and higher-order multipole plasmon resonances, agreeing reasonably well with experimental results. The characteristic peaks observed at 650 and 600 nm in Figure 3a can then be assigned, respectively, to quadrupole and octopole plasmon modes, and the broadband at ~800−900 nm can be assigned to the dipole mode. The differences in plasmon peak positions and shapes between observed and calculated spectra can be ascribed to the broad size distribution of the prepared nanocrystals.

It has been generally known that the shape of noble metal nanocrystals can be modulated by controlling the reduction kinetics of metal precursors and relative growth rate on particular crystallographic surfaces during the crystal growth.[9] In our experiment, DMF acts both as a solvent and as a reducing agent. In the previous studies on the formation of Ag nanocrystals, Liz-Marzán et al. found that DMF is a powerful reductant and the reduction rate remarkably increases as the temperature increases.[15] The optimal temperature for the synthesis of homogeneous nanocrystals was found to be the boiling point of DMF, i.e., 156 °C. In our experimental conditions, the reaction temperature was maintained at 90−95 °C well below the boiling temperature of DMF, therefore leading to a relatively slow rate of crystal growth. This kinetically controlled reduction process should contribute to the formation of the rhombic dodecahedral Au nanocrystals. When the reaction temperature was increased above 90−95 °C, rhombic dodecahedral particles were not produced; instead, variously shaped polyhedral particles were formed (Figure S2). On the other hand, the formation of rhombic dodecahedral nanocrystals with exposed high-energy {110} surfaces may also be the result of stabilization of such unstable facets by DMF or one of its oxidation products. This was confirmed by the fact that we could not obtain the rhombic dodecahedral nanocrystals when we added poly(vinyl pyrrolidone) (PVP) into the reaction mixture as a competing stabilizer (Figure S3). PVP known as the surface-regulating polymer is believed to preferentially adsorb on the {111} planes of Au nanocrystals, reduce the growth rate along the [111] direction, and finally result in the formation of nanocrystals enclosed by {111} surfaces.[4,5]

In summary, we have presented the synthesis method for the production of rhombic dodecahedral Au nanocrystals bound by 12 {110} facets. The exposed high-energy {110} surfaces of the nanocrystals will benefit a variety of optical and catalytic applications. For instance, a preliminary experiment shows that the prepared nanocrystals exhibit efficient surface-enhanced Raman scattering properties (Figure S4).

Acknowledgment. This work was supported by grants from the MEST/KOSEF to the Environmental Biotechnology National Core Research Center (Grant No. R15-2003-012-01001-0), EPB Center (Grant No. R11-2008-052-02003), and Pioneer Research Center for Nanomorphic Biological Energy Conversion and Storage. Q.P. is supported by KRF/KOSEF.

Supporting Information Available: Experimental and calculation details. Figures S1−S4. This material is available free of charge via the Internet at http://pubs.acs.org.

References

(1) (a) Burda, C.; Chen, X.; Narayanan, R.; El-Sayed, M. A. *Chem. Rev.* **2005**, *105*, 1025. (b) Xia, Y.; Halas, N. J. *Mater. Res. Soc. Bull.* **2005**, *30*, 338. (c) Rosi, N. L.; Mirkin, C. A. *Chem. Rev.* **2005**, *105*, 1547.
(2) Xiong, Y.; Wiley, B. J.; Xia, Y. *Angew. Chem., Int. Ed.* **2007**, *46*, 7157.
(3) (a) Tian, N.; Zhou, Z.; Sun, S.; Ding, Y.; Wang, Z. L. *Science* **2007**, *316*, 732. (b) Ma, Y.; Kuang, Q.; Jiang, Z.; Xie, Z.; Huang, R.; Zheng, L. *Angew. Chem., Int. Ed.* **2008**, *47*, 8901.
(4) Kim, F.; Connor, S.; Song, H.; Kuykendall, T.; Yang, P. *Angew. Chem., Int. Ed.* **2004**, *43*, 3673.
(5) Li, C.; Shuford, K. L.; Park, Q.-H.; Cai, W.; Li, Y.; Lee, E. J.; Cho, S. O. *Angew. Chem., Int. Ed.* **2007**, *46*, 3264.
(6) Sánchez-Iglesias, A.; Pastoriza-Santos, I.; Pérez-Juste, J.; Rodríguez-González, B.; García de Abajo, F. J.; Liz-marzán, L. M. *Adv. Mater.* **2006**, *18*, 2529.
(7) Kwon, K.; Lee, K. Y.; Lee, Y. W.; Kim, M.; Heo, J.; Ahn, S. J.; Han, S. W. *J. Phys. Chem. C* **2007**, *111*, 1161.
(8) Sun, Y.; Xia, Y. *Science* **2002**, *298*, 2176.
(9) Tao, A. R.; Habas, S.; Yang, P. *Small* **2008**, *4*, 310.
(10) Wang, Z. L. *J. Phys. Chem. B* **2000**, *104*, 1153.
(11) (a) Liu, X.; Wu, N.; Wunsch, B. H., Jr.; Stellacci, F. *Small* **2006**, *2*, 1046. (b) Montejano-Carrizales, J. M.; Rodrı´guez-López, J. L.; Pal, U.; Miki-Yoshida, M.; José-Yacamán, M. *Small* **2006**, *2*, 351. (c) Niu, W.; Zheng, S.; Wang, D.; Liu, X.; Li, H.; Han, S.; Chen, J.; Tang, Z.; Xu, G. J. Am. Chem. Soc. 2009, DOI: 10.1021/ja804115r.
(12) Xiang, Y.; Wu, X.; Liu, D.; Feng, L.; Zhang, K.; Chu, W.; Zhou, W.; Xie, S. *J. Phys. Chem. C* **2008**, *112*, 3203.
(13) Williams, D. B.; Carter, C. B. *Transmission Electron Microscopy: A Textbook for Materials Science*; Plenum Press: New York, 1996; Chapter 18.
(14) Draine, B. T.; Flatau, P. J. *J. Opt. Soc. Am. A* **1994**, *11*, 1491.
(15) (a) Pastoriza-Santos, I.; Liz-Marzán, L. M. *Langmuir* **1999**, *15*, 948. (b) Pastoriza-Santos, I.; Liz-Marzán, L. M. *Nano Lett.* **2002**, *2*, 903.

JA809112N